Journal of Materials Chemistry A

Insights into the Extraction of Photogenerated Holes from CdSe/CdS Nanorods for Oxidative Organic Catalysis

Journal:	*Journal of Materials Chemistry A*
Manuscript ID	TA-ART-02-2021-001124.R1
Article Type:	Paper
Date Submitted by the Author:	13-Apr-2021
Complete List of Authors:	Sha, Yuchen; Wuhan University, College of Chemistry & Molecular Sciences Lin, Xiao-Min; Argonne National Laboratory, Materials Science Division; Bldg. 200 Niklas, Jens; Argonne National Laboratory, Chemical Sciences & Engineering Poluektov, Oleg; Argonne National Laboratory, Chemical Sciences and Engineering Division Diroll, Benjamin; Argonne National Laboratory, Center for Nanoscale Materials Lin, Yulin; Argonne National Laboratory, Center for Nanoscale Materials Wen, Jianguo; Argonne National Laboratory, Electron Microscopy Center Hood, Zachary ; Argonne National Laboratory, Lei, Aiwen; Green Catalysis Institute, The College of Chemistry and Molecular Sciences Shevchenko, Elena; Argonne National Laboratory, Center for Nanoscale Materials

ARTICLE

Insights into the Extraction of Photogenerated Holes from CdSe/CdS Nanorods for Oxidative Organic Catalysis

Received 00th January 20xx,
Accepted 00th January 20xx

DOI: 10.1039/x0xx00000x

Yuchen Sha, [a, b] Xiao-Min Lin,[b,] * Jens Niklas, [c] Oleg G. Poluektov, [c] Benjamin T. Diroll, [b] Yulin Lin, [a, b] Jianguo Wen, [b] Zachary D. Hood,[d] Aiwen Lei, [a,]* and Elena V. Shevchenko [b,e]*

Using aerobic oxidative coupling of thiolphenol in organic media as a model reaction, we show that photogenerated holes in CdSe/CdS core-shell nanorods can be efficiently exctracted. As a result, CdSe/CdS nanorods can serve as an efficient visible-light photocatalyst at a very low concentration (~1.5×10^{-4} mol%). We show that primary amines play an important role in the transformation of thiols into disulfides by forming a soluble thiolate in nonpolar solvent. Using time-resolved optical spectroscopy and electron paramagnetic resonance spectroscopy, we show thiolate can efficently extract the photogenerated holes from CdSe/CdS nanorods and transform into disulfide in organic solven. Our data indicate that there are two reaction pathways responsible for of S-S coupling of thiolate upon illimination of CdSe/CdS nanorods. We demonstrate that instead of scavenging of photogenerated holes by sacraficial species for preventing of photo corrosion of CdSe/CdS nanorods, the photogenerated holes can be efficiently used for oxidative organic synthesis.

Introduction

Semiconductor nanocrystals (NCs) have been extensively studied for applications in photocatalysis.[1-7] As compared to metal complex based photocatalysts and molecular dyes, they have higher optical extinction coefficients and can be easier separated from the reaction products.[8] CdSe/CdS nanorods (NRs) with CdSe core and CdS shell provide an excellent opportunity to maximize the solar absorption and convert a broad range of visible spectrum to chemical energy.[9, 10] Tuning the diameter of CdSe core and the volume of CdS shell can generate a quasi- type-II semiconductor heterostructure, in which photo-excited holes are confined within the CdSe core and electrons are delocalized.[11-13] The spatial separation of the electrons and holes reduces the recombination rate and increases the probability of carries to be extracted.[14, 15] This characteristics of CdSe/CdS NRs inspired a number of photocatalytic studies aiming at utilizing electrons in reductive reactions.[14, 16-18] These initial photocatalytic studies on cadmium chalcogenides heterostructures were mainly conducted in aqueous media (e.g., hydrogen generation), with holes scavenged by sacrificial electron donors to prevent oxidation of semiconductor NCs.[3, 14, 16-22] Utilizing photogenerated charge carriers, both electrons and holes, could lead to synthesis of a broad range of high value products in organic solvents.[8, 23-26] Recent reports demonstrate a number of promising reactions, including aerobic oxidation of aliphatic boronic acid,[23] transformation of diazonium salt to arylboronate,[24] and β-alkylation of aldehyde.[25] However, these studies are only limited to spherical CdSe and CdS NCs. In comparison, CdSe/CdS NRs should have better photocatalytic capability due to a better charge separation of the photogenerated holes and electrons as described above. One concern to utilize them in oxidative reaction is whether the holes localized at CdSe core can be efficiently extracted. Several recent studies on CdSe/CdS NRs indirectly suggest a rather efficient hole removal process do occur, as sacrificial species could effectively protect CdSe/CdS heterostructure from oxidation.[18, 19, 22] Also, it was shown that H_2 generation depends on the efficiency of the hole extraction.[19, 27] These observations point to the possibility of utilizing hole extraction from CdSe/CdS NRs in valuable oxidative photocatalytic reactions.

Here, we present detailed insights into utilization of CdSe/CdS NRs as an oxidative photocatalyst in a nonpolar solvent using S-S coupling of thiophenol as a model reaction. We choose this reaction because the transformation of thiol into disulfide is an important reaction for many biological processes, responsible for folding many peptides and proteins into biologically active conformations.[28, 29] Also, disulfides are extensively utilized in fine chemical synthesis and can be used to produce a broad class of materials ranging from antioxidants, pharmaceuticals, pesticides to rubber vulcanization agents.[30]

Many previously reported photocatalytic studies on disulfide synthesis used a relatively high homogenous catalyst

[a.] *Institute of Advanced Studies (IAS), College of Chemistry and Molecular Sciences, Wuhan University, Wuhan 430072, Hubei, P. R. China.*
[b.] *Center for Nanoscale Materials, Argonne National Laboratory, Argonne, Illinois, 60439 USA.*
[c.] *Chemical Sciences and Engineering Division, Argonne National Laboratory, Argonne, Illinois, 60439 USA*
[d.] *Applied Materials Division, Argonne National Laboratory, Argonne, Illinois, 60439 USA*
[e.] *Department of Chemistry and James Frank Institute, University of Chicago, Chicago, Illinois, 60637 USA*
* *E-mails: Xiao-Min Lin (xmlin@anl.gov), Aiwen Lei (aiwenlei@whu.edu.cn), Elena Shevchenko (eshevchenko@anl.gov)*
† Electronic Supplementary Information (ESI) available: See DOI: 10.1039/x0xx00000x

loading to achieve a reasonable reaction conversion (>80 % in 3 – 12 h), i.e., $Ir(ppy)_3$ (>0.5 mol%),[31] diaryl tellurides (1 mol%),[32] $Mn(CO)_5Br$ (5mol%),[33] Eosin Y (1 mol%),[34] and Rose Bengal (5 mol%),[35]. Recently, S-S coupling reactions were conducted using semiconductor nanostructures in order to avoid the laborious process of catalyst separation in homogeneous catalysis.[36] However, in those cases, the catalyst-loadings were still relatively high, i.e. CdSe (0.04 mol%)[37] and $CsPbX_3$ (1.0 mol%).[38]

We show that CdSe/CdS NRs can serve as an efficient visible light photocatalyst in aerobic oxidative coupling reaction, transforming thiol to disulfide in toluene with catalyst loading at a minuscule level. We demonstrate that primary amines play an important role in this process via forming soluble thiolates in nonpolar solvents, which is much more efficient than thiol in extracting holes from CdSe/CdS NRs. Time dependent optical spectroscopy as well as electron paramagnetic resonance (EPR) reveal two major reaction pathways that are responsible for the synthesis of disulfides from thiolates: (i) a direct photooxidation by oxygen and (ii) an oxidation of thiolate by photogenerated holes through NRs. We achieved a ~87% yield of disulfide from thiophenol in 2 hours in the presence of CdSe/CdS NRs at only ~1.5×10^{-4} mol%, with ~31% of disulfide originated from the direct photooxidation of thiolate. The apparent quantum yield of the photocatalytic thiophenol oxidation in the presence of CdSe/CdSe NRs is estimated to be ~52%. Our finding opens up the possibility of utilizing photogenerated holes for efficient synthesis of other valuable compounds in organic media.

Results and Discussions

Performance of CdSe/CdS NRs in oxidative S-S coupling. CdSe/CdS NRs (Fig. 1a, S1, S2) were prepared according to a previously reported method.[9, 10] Transmission electron microscopy (TEM) analysis showed the obtained CdSe/CdS NRs were on average 3.9 nm wide and 28.4 nm long. This dimension was chosen to optimize the absorption of light by a relatively large volume of CdS shell, but still with a relative thin coating on the CdSe core (~0.4nm). Detailed synthesis steps, X-ray diffraction (XRD) and X-ray photoelectron spectroscopy (XPS) analysis are described in the Experimental Section and the Supporting Information.

The oxidative S-S coupling of thiophenol (**1a** in Table 1) was investigated using a blue LED light (415 nm, 14.4 mW power) in a toluene solution with CdSe/CdS NRs as photocatalysts. Since surface ligands can hinder the access of substrate molecules to the catalytic surface, we washed the as-prepared CdSe/CdS NRs with methanol three times. The photocatalytic reaction of thiophenol was carried out under ambient conditions (room temperature, air) in the presence of washed NRs, and the formation of disulfide (product **2a**) observed in 2 h was at 33% yield (Table 1, entry 1; blue curve in Fig. 1b). No disulfide was formed without CdSe/CdS NRs (Table 1, entry 2). This observation reveals that photogenerated holes can be extracted and used for photo-oxidative S-S coupling. However, the reaction was accompanied by an increase of the turbidity of the reaction mixtures (Fig. 1c), which is a result of an agglomeration of CdSe/CdS NRs. Therefore, we added a primary amine to increase the colloidal stability of semiconductor NRs.[39] Introducing of a small amount of *n*-octylamine (0.02 M) not only improved the stability of CdSe/CdS NRs (Fig. 1d) but also resulted in a higher yield of disulfide (42%, Table 1, entry 3). Further increase of *n*-octylamine concentration up to the stoichiometric equivalent of thiophenol led to 87% yield in 2 h (Table 1, entry 4; black curve in Fig. 1b). This reaction condition that allowed the highest yield of disulfide was chosen as a standard, and we used it in all further tests discussed below unless specified otherwise. The apparent quantum yield of this reaction under this condition is ~52% (see Supporting Information). Further increase of the reaction time (up to 6 h) did not lead to a significant change in the yield of disulfide.

Since holes are localized in CdSe core, we anticipated that there might be a difficulty in extracting them from CdSe/CdS

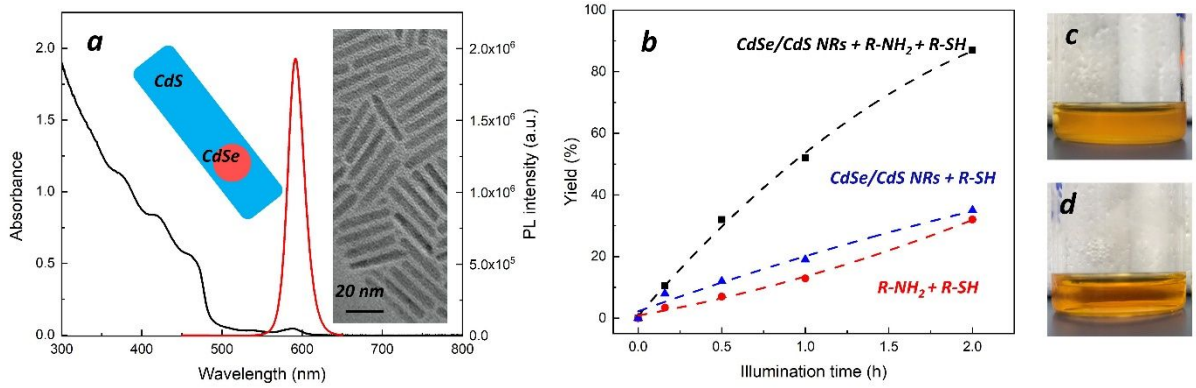

Fig. 1 (a) UV/Vis absorption and photoluminescence (PL) spectra of 3.9 nm wide and 28.4 long CdSe/CdS NRs with 3.1 nm CdSe cores. Inset in (a) shows the TEM image of CdSe/CdS NRs. (b) Time dependence of disulfide yield for three different reaction conditions: Entry 4 in Table 1 with CdSe/CdS NRs, thiophenol and *n*-octylamine (black squares); Entry 1 in Table 1 with CdSe/CdS NRs and thiophenol (blue triangles), and entry 6 in Table 1 with thiophenol and *n*-octylamine (red dots). Dash lines are guide for the eye. All experiments were conducted under ambient conditions in 2 mL of toluene using 415 nm LED light. The concentrations of thiophenol and *n*-octylamine were 0.1 M each. The concentration of CdSe/CdS NRs was 1.5×10^{-7} M (~1.5×10^{-4} mol%). Optical images demonstrating that the addition of *n*-octylamine improves the stability of CdSe/CdS NRs against agglomeration in reaction media during photocatalytic test (c and d correspond to reaction mixture after 2 h photocatalytic test without and with *n*-octylamine, respectively).

NRs. However, our experimental results indicate that CdSe/CdS NRs outperformed CdSe QDs under the same molar conditions (Table 1, entry 5). The yield of disulfide using CdSe NCs (39%) is significantly lower than CdSe/CdS NRs (87%). It is important to note that, with no CdSe/CdS NRs but using *n*-octylamine concentration equivalent to that of thiophenol, disulfide can still be formed with a 31% yield in 2 h (Table 1, entry 6; red curve in Fig. 1b). In fact, this yield of disulfide (31%) is comparable with the 39% yield of disulfide obtained with CdSe NCs. These data indicate that (i) *n*-octylamine can promote S-S coupling reaction on its own, and (ii) CdSe NCs is not a very active photocatalyst in an aerobic S-S coupling reaction.

In contrast to previous studies on S-S coupling by CdSe NCs in water[37] and perovskite NCs in organic solvents,[38] only trace amount of disulfide **2a** were obtained in the presence of CdSe/CdS NRs when the reaction was conducted under N_2, without light or under a green LED light (Table 1, entries 7, 8 and 9). It is worth noting that CdSe/CdS NRs demonstrated some catalytic activity even at a very small concentration (Table 1, entry 10). Finally, changing the length of the CdSe/CdS NRs to 113 nm (Fig. S3) did not change the apparent yield of the product under the identical experimental conditions. (Table 1, entry 11). No overoxidation products, such as sulfenic acid (RSOH), sulfinic acid (RSO_2H), sulfonic acid (RSO_3H) or their deprotonated forms, were detected.[40, 41]

Table 1. Effect of the reaction conditions on the disulfide yield.

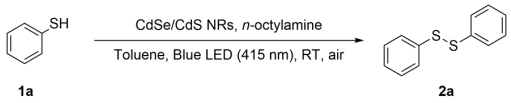

1a 2a

Entry	variation of standard condition	yield (%) [b]
1	no *n*-octylamine	33
2	no *n*-octylamine and no CdSe/CdS NRs	No reaction
3	0.02 M *n*-octylamine	42
4[a]	none	87
5	CdSe instead of CdSe/CdS NRs	39
6	no CdSe/CdS NRs	31
7	under N_2	Trace
8	under dark	Trace
9	under green LED	Trace
10	CdSe/CdS NRs (3.75×10^{-5} mol%)	44
11	CdSe/CdS NRs (~113 nm)	89

[a] Standard condition (entry 4): thiophenol (0.2 mmol), *n*-octylamine (0.2 mmol), CdSe/CdS NRs (1.5×10^{-4} mol%), and toluene (2.0 mL) under 415 nm blue LED light and air at room temperature. [b] The reaction yield was determined by GC-MS using biphenyl as an internal standard. Each experiment was conducted at least three times. The deviation of each result was within 5%.

Hole extraction probed by photoluminescence and time dependent optical spectroscopy. In order to explore the mechanism of S-S coupling by CdSe/CdS NRs and the role of amine, we investigated the effect of thiophenol and *n*-octylamine on the optical properties of CdSe/CdS NRs. We observed that the addition of *n*-octylamine resulted in a slight enhancement in the photoluminescence (PL) intensity (red curve in comparison to black curve in Fig. 2a) that is consistent with a better surface passivation of NRs in the presence of extra alkylamine.[42] Introducing thiophenol to the solution of CdSe/CdS NRs led to a significant decrease of the PL intensity (blue curve, Fig. 2a) that is in agreement with the previously reported PL quenching in the presence of hole accepting ligands.[43, 44] PL is quenched slightly more when both thiophenol and *n*-octylamine are present (green curve in in Fig. 2a).

To understand the effects of ligands further, we studied time-resolved PL decays[27, 43, 45, 46] of CdSe/CdS NRs before and after adding thiophenol, *n*-octylamine, and their mixture. PL

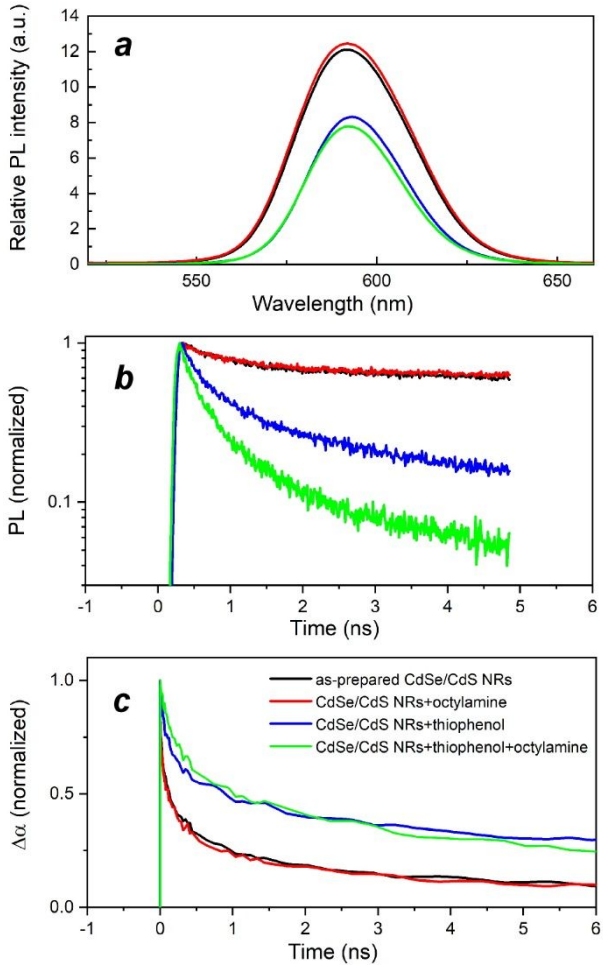

Fig. 2 (a) PL spectra, (b) time-resolved photoluminescence decays and (c) ultrafast transient absorption (TA) decays of CdSe/CdS NRs (black curve), with *n*-octylamine only (red curve), with thiophenol only (blue curve), and with both thiophenol and *n*-octylamine (green curve).

photons were spectrally dispersed and detected using a streak camera.[12, 47] The time-resolved PL decay behavior of CdSe/CdS NRs does not change in the presence of *n*-octylamine (black and red curves in Fig. 2b). The fast kinetics of the initial PL decay likely corresponds to the carrier trapping.[47] The drastically accelerated decay of PL in the presence of thiophenol indicates that a new PL quenching route is available (blue curve, Fig. 2b), which is suggestive of a hole transfer process between photoexcited CdSe/CdS and thiophenol. In turn, *n*-octylamine makes this charge transfer much more efficient (green curve, Fig. 2b).

Assignment to a hole transfer process is reinforced by ultrafast transient absorption (TA) spectroscopy[48-50] under the same excitation conditions (Fig. 2c). Due to the smaller electron effective mass and small conduction band offset, TA dynamics measured at 455 nm monitor the dynamics of photoexcited electrons in the CdS shell, whereas PL dynamics are sensitive to both electrons and holes. We found that *n*-octylamine alone did not affect the electrons' dynamics in CdSe/CdS NRs (black and red curves in Fig. 2c). Adding thiophenol, TA decays become longer, indicating that electrons remain in CdS shell longer as compared to as-synthesized CdSe/CdS NRs or with *n*-octylamine alone (blue and green curves in Fig. 2c). The observation of longer-lived electrons in CdS shell in the presence of thiophenol supports the assignment of hole transfer to thiophenol from PL decay (Fig. 2b). This observation also confirms that hole extraction can affect the electron transfer processes, as it was previously observed that photocatalytic H_2 generation is highly dependent upon the efficiency of the hole extraction from CdSe/CdS NRs.[27] A longer lifetime of photo-excited electrons also increases the probability of these electrons to be extracted by electron scavengers.[27] The PL dynamics behavior is consistent with the trend of PL decrease (Fig. 2a) and higher yields of disulfide in the presence of *n*-octylamine (Table 1). The possible explanation of these results could be related to the different oxidation potentials of thiols and thiolates and their relative positions with respect to valence band (VB) potential of CdSe/CdS NRs (*vide infra*). [20, 51]

The reactive intermediates probed by electron paramagnetic resonance (EPR). Previous studies suggest that photocatalytic oxidative coupling of aromatic thiols in water occurred via the formation of thiyl radicals.[52] To understand the mechanism of the oxidative S-S coupling catalyzed by CdSe/CdS NRs in organic solvents and characterize paramagnetic intermediates (radicals), we resorted to EPR technique. The samples for EPR experiments were prepared by freezing the reaction mixtures at 10K to increase the probability of detecting paramagnetic intermediates. We found that when excited by a blue (440 nm) laser, the solution containing thiophenol and *n*-octylamine

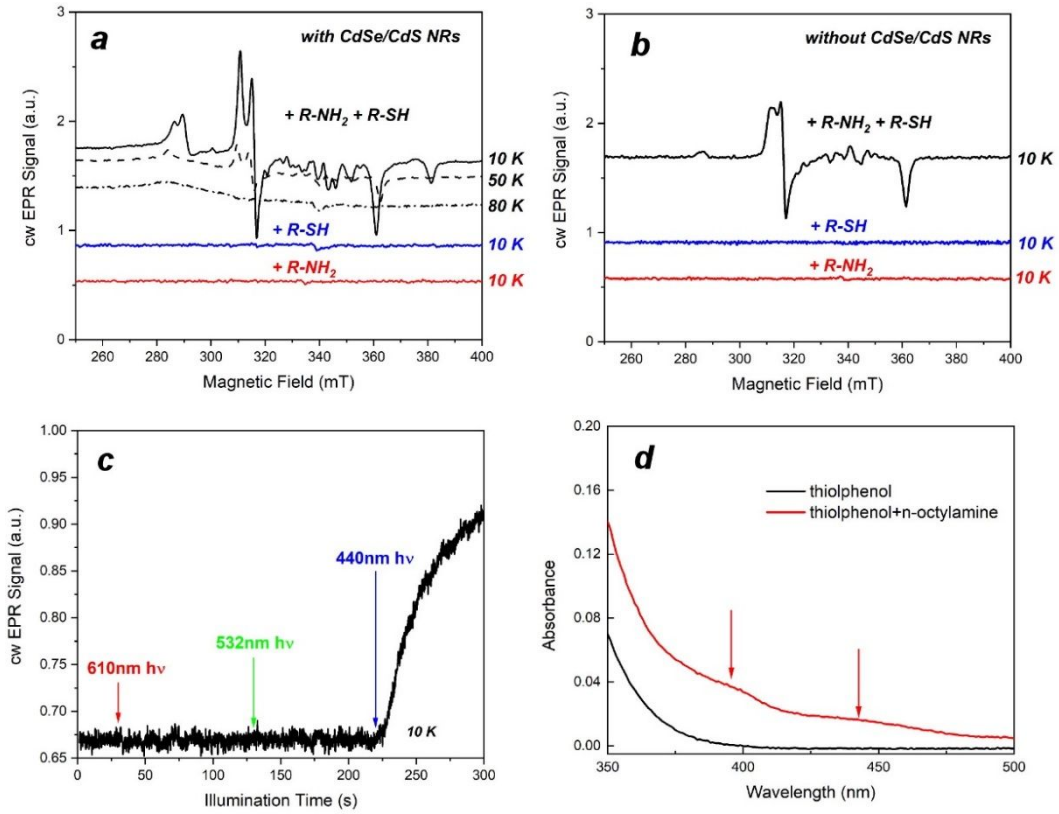

Fig. 3 (a) EPR spectra from a reaction mixture that contains CdSe/CdS NRs, thiophenol and *n*-octylamine. Data were acquired at different temperatures 10 K (solid black), 50 K (dash black) and 80K (dash-dot black). EPR spectra for CdSe/CdS NRs with thiophenol only (blue); CdSe/CdS NRs and *n*-octylamine only (red). (b) EPR spectra acquired at 10 K from a mixture of thiophenol and *n*-octylamine without CdSe/CdS NRs, a solution that contains thiolphenol only (blue) and a solution that contains *n*-octylamine only (red). (c) EPR signals of a solution containing CdSe/CdS NRs, thiophenol and *n*-octylamine acquired at 10 K under different wavelengths of illumination. (d) UV/Vis spectra of thiophenol (black) and a mixture of thiophenol and *n*-octylamine (red). The composition of different components is the same as used in photocatalytic reaction.

showed an EPR spectrum with a complex pattern of well-resolved peaks, regardless whether it contains CdSe/CdS NRs or not (Fig. 3a-b), only the signal is slightly weaker in the absence of NRs. These peaks in EPR spectra are indicative of the presence of paramagnetic species. They do not appear when the reaction mixture is kept in the dark or illuminated by green or red lasers (Fig. 3c). These results are consistent with the data of the catalytic tests revealing that only trace amounts of disulfide are formed in the dark or under a green LED irradiation (Table 1, entries 8 and 9). Under the identical conditions, regardless whether the solution contains CdSe/CdS NRs or not, if only thiophenol is present (blue curve), or only *n*-octylamine is present (red curve), the EPR spectra appeared to be featureless (Fig. 3a-b).

The complex structure of the EPR signals imposes a challenge to identify the precise structure of the paramagnetic intermediates. However, based on the peak positions, it is reasonable to suggest that the signal belongs to the S-centered radicals.[53] The increase of the temperature results in a decrease in the intensities of the EPR signals (dash and dash-dotted curves in Fig. 3a). No EPR peaks are observed at 80K. These results indicate that photogenerated S-centered radicals are in a transient state that are unstable at a higher temperature. Based on the pKa values of thiophenol and *n*-octylamine, the interaction of thiols and amines can lead to the formation of alkylammonium thiolate.[54] The formation of alkylammonium salts of mercaptans was proposed to explain the catalytic effect of aliphatic amines in the reaction of chemical oxidation of mercaptans and hydroperoxides into corresponding disulfides and alcohols.[55] When mixing thiophenol and *n*-octylamine in toluene, we observed an instantaneous formation of a white solid that is consistent with the formation of alkylammonium thiolate salt reported earlier.[55] However, this white precipitate quickly re-dissolves, suggesting that thiolate salt is soluble in toluene at the concentration we used in photocatalytic reaction.

The thiolate formation was previously found to be a critical process in photooxidative S-S coupling of *p*-nitrothiophenol in water.[56] The maximum yield of disulfide in water was achieved by excitation of the anionic thiolate form of *p*-nitrothiophenol at 455 nm at pH ~5, at which both thiol and thiolate forms are present.[56] However, the exact mechanism of photooxidative S-S coupling of thiols remains unclear. In the case of p-nitrothiophenol, the formation of its thiolate in water is accompanied by a pronounced absorption peak at ~441 nm. The number of peaks and their positions were found to depend on the solvent.[56] In nonpolar toluene solution, our UV/Vis data indicate that the addition of *n*-octylamine to thiophenol also results in the low-intensity peaks at ~440 nm and at ~390 nm that are indicative of thiolate formation (Fig. 3d).[56] These structures can absorb light, which facilitates a rather high yield of disulfide (~31%) even in the absence of CdSe/CdS NRs (Table 1, entry 6). Since aerobic condition is critical to this reaction, we expect that O_2 could play a pivotal role as an electron scavenger.

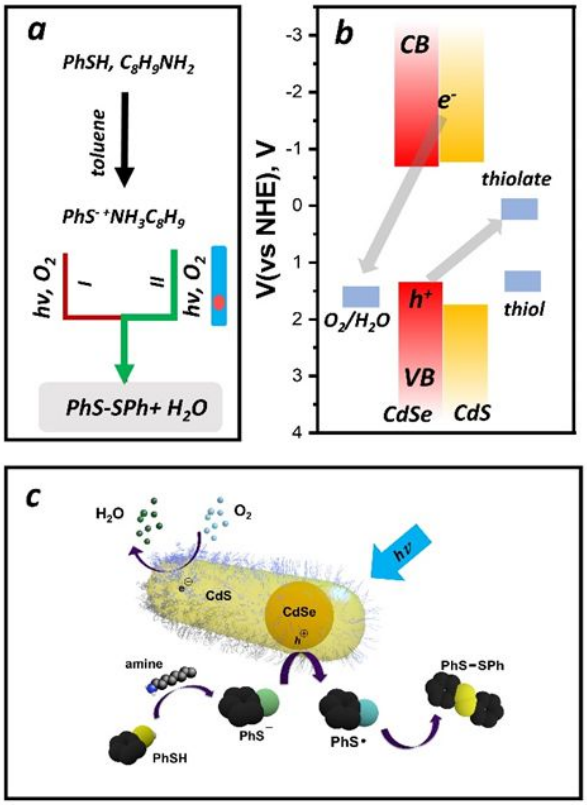

Fig. 4 (a) Summary of two different pathways for photooxidation of thiolphenol in the presence of *n*-octylamine (b) The relative band alignment of CdSe/CdS NRs, the position of the redox potentials of the thiophenol, its thiolate form, and O_2/H_2O in organic solvent. (The broad lines depict the range of redox potentials calculated using the redox potentials reported for internal ferrocene/ferrocenium redox electrode). (c) A schematic diagram that illustrate the reaction pathway II: disulfide formation promoted by the hole transfer process from the core of CdSe/CdS NRs.

Reaction Mechanism. The results of photocatalytic studies, optical and EPR spectroscopy data described above point to a conclusion that there are two photoreaction pathways when *n*-octylamine is involved, as depicted in Fig. 4a. Pathway I takes place in the absence of CdSe/CdS NRs, in which the light-driven synthesis of disulfide occurs directly with a yield of 31% (Table 1, entry 6). We attribute this to the fact that mixing thiophenol and octylamine results in the formation of thiolate that adsorbs light at 415 nm (Fig. 3d). Based on the positions of the redox potentials measured for thiolate and H_2O/O_2 in organic solvents (Fig. 4b), we can conclude that its oxidation by oxygen is possible. It should be noted that the pathway I is consistent with the previously reported oxidation of thiol by molecular oxygen in the presence of nitrogen containing species.[55, 57] It is reasonable to expect that this reaction pathway can still contribute to the total yield of disulfide even when CdSe/CdS NRs are used. The presence of CdSe/CdS NRs, on the hand, creates a new reaction pathway. The small band offset between the conduction band in CdSe core and CdS shell lead to the delocalization of photogenerated electrons inside the CdS shell, while holes are trapped inside the CdSe core, a scenario known as quasi-type II band alignment.[12] The spatial separation of photogenerated charges slows down the recombination

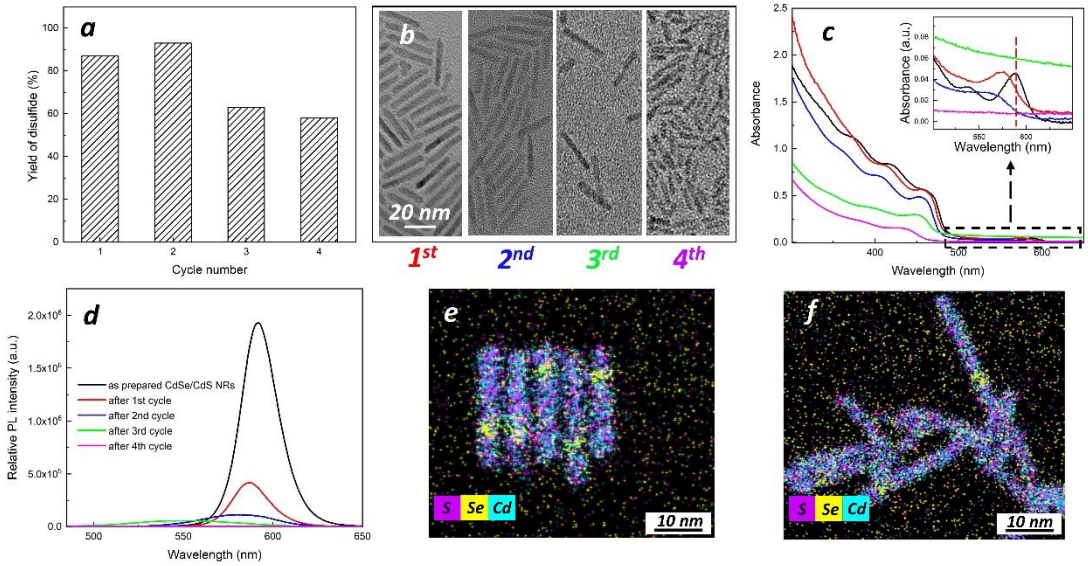

Fig. 5 (a) Photocatalytic recyclability performance of CdSe/CdS NRs in oxidative coupling reaction of thiophenol; (b) TEM images of CdSe/CdS NRs after each catalytic cycle; (c) UV/Vis and (d) PL spectra of CdSe/CdS NRs before and after each photocatalytic test cycle. The black, red, blue, green and magenta spectra correspond to toluene solutions of CdSe/CdS NRs before reaction and after first, second, third and fourth cycles, respectively. Elemental mapping images of CdSe/CdS NRs before 1st (e) and after 4th (f) photocatalytic cycles, reconstructed from the false color superposition of S (magenta), Se (yellow) and Cd (cyan) obtained from a scanning transmission electron microscopy (STEM) equipped with an energy dispersive X-ray spectrometer (EDXS).

process, which allows thiolates to extract the photogenerated holes more efficiently from CdSe cores, creating phenylthiyl radicals that further dimerize into disulfide (pathway II, Fig. 4a). In organic nonpolar solvent the amines can thus play the same role as pH in aqueous solution, regulating the thiolate formation. Electrochemical studies revealed that thiols have more higher positive redox potential than corresponding thiolates.[51, 58] Therefore, the addition of amines lowers the redox potential of thiol facilitating its oxidation by photogenerated holes enabling 87% yield of disulfide (Table 1). The pathway II is responsible for 56% of disulfide yield. It is also intriguing that CdSe/CdS NRs allow 33% yield of disulfide from thiophenol even without adding octylamine (Table 1, entry 1). The redox potential of thiol is close to or slightly lower than the position of the valence band of CdSe/CdS estimated electrochemically in organic solvents (Fig. 4b). Therefore, the hole transfer to thiols is possible, but not very efficient. Part of the thiol molecules also likely deprotonate when they bind to the surface,[59] which results in a more negative redox potential and hence facilitate the hole transfer.

Previous studies revealed hole diffusion and trapping processes are highly efficient in CdS and CdSe/CdS NRs.[11, 27] In CdSe/CdS NRs, CdSe core can trap holes on the time scale of picosecond.[11, 60] However, the exciton localization efficiency, which is the ratio between amount of excitons migrate and trapped near the core vs the initial photogenerated excitons, depend upon the length of the nanorod. For 29 nm long CdSe/CdS NRs, it was reported to be ~75 % and for 113 nm CdSe/CdS NRs it was found to be ~30.5%.[11] As compared to picosecond trapping of photogenerated holes in CdSe/CdSe NRs at CdSe core, their extraction from CdSe core by thiolate is a much slower process. Time-resolved PL decay measurements in Fig. 2b shows that the hole extraction occurs on the order of nanosecond. Under constant illumination, the amount of photogenerated holes is abundant, and the hole extraction is likely to be the bottleneck process that controls the reaction rate. Therefore, it is not too surprising that we observed that 29 nm and 113 nm CdSe/CdS NRs gave nearly the identical reaction yield after two hours (Table 1, entry 10).

The photogenerated electrons delocalized in CdS shell are likely transferred to oxygen, reducing it to water. Analysis of the band positions of CdS/CdSe and redox potential of O_2/H2O in organic solvent points out that the reduction of O_2 to H_2O is a feasible reaction (Fig. 4b). (Note, that we used redox potentials reported for thiophenol, its thiolate form, and oxygen in organic solvents. [51, 61] More details are described in the Supporting Information.) The formation of water as a result of aerobic oxidation is a common reductive reaction that accompanies oxidative S-S coupling reaction.[25, 62, 63] Under anaerobic conditions in water semiconductor NCs allow the synthesis of H_2 as a result of electron scavenging by protons.[37] In toluene solution, there is no source of protons and, hence, under aerobic conditions, the electron transfer to O_2 is the more likely process (Fig. 4c). This also explains no formation of disulfide under anaerobic conditions (Table 1, entry 7).

According to previous studies, four electron process of H_2O formation is considered to be a more thermodynamically favorable process as compared to the two electron process that is responsible for H_2O_2 formation.[64-67] However, whether H_2O or H_2O_2 form depends on how oxygen bounds to the catalyst surface.[67, 68] Previously it was demonstrated that reactive oxygen species (ROS), such as superoxide radical anion (OO-•) and hydrogen peroxide, could also form during the electron transfer from CdSe/CdS NRs in water.[69] Since H_2O_2 was reported

to oxidize both neutral thiol and thiolate into disulfide,[40, 41] it is thus important to understand whether thermodynamically favorable four electron formation of H_2O or two electron formation of H_2O_2 takes place upon extraction of electrons by O_2. In a controlled experiment, we added H_2O_2 aqueous solution (0.1M) directly into in a toluene solution of thiolphenol and *n*-octylamine, which resulted in nearly 100% conversion of thiolate into disulfide. However, even 0.02M H_2O_2 would cause a dramatic change of CdSe/CdS nanorods within minutes, strongly affecting their morphology and optical properties (Fig. S4 in Supporting Information). Because the partition coefficient of H_2O_2 in organic solvent is low,[70] the actually amount of H_2O_2 in toluene is much lower than the amount we have added. The fact in our photocatalytic reaction in toluene, CdSe/CdS are stable for hours under light proves that intermediate reactive oxygen species such as peroxide are not produced in any significant quantity. Direct detection of the OO-• by EPR spectroscopy is challenging (see Supporting Information). But the presence of OO-• would lead to oxidation of thiol and generate H_2O_2 in the process,[71] which, in turn, have the same detrimental effect on the stability of NRs. These experiments indicate that photogenerated electrons are consumed in oxygen reduction, forming water as a major product.

Stability and recyclability of the catalyst. To estimate the stability of CdSe/CdS NRs as photocatalyst in the oxidative S-S coupling reaction, we cycled the same CdSe/CdS NRs four times under the identical reaction conditions. After each 2 h reaction, the catalyst was precipitated by the acetone, isolated by centrifugation and re-dispersed in a fresh reaction solution. The yield of disulfide in the second cycle was slightly higher than the first one (Fig. 5a). TEM analysis of CdSe/CdS NRs indicates that no detectable change can be found after the first 2 h reaction cycle (Fig. 5b), which is in agreement with the optical spectroscopy data (Fig. 5c). Some increase in activity of CdSe/CdS NRs in the second cycle can be a result of further removal of ligands (TOPO and TOP) that sterically hinder the catalytic surface. However, further cycling of CdSe/CdS NRs resulted in an apparent decrease in their catalytic activity (Fig. 5a), possibly due to loss of surface ligand and the presence of trace amount of ROS created by oxygen reduction process, as we discussed above.

The UV/Vis and PL spectra acquired for CdSe/CdS NRs before and after each catalytic cycle demonstrate a blue shift of peaks characteristic to CdSe and CdS after catalytic reactions (Fig. 5c and 5d). The intensities of the UV/Vis spectra of the samples recovered after catalytic tests also decrease after each cycle. The PL spectra demonstrate a significant decrease in PL intensities (Fig. 5d). Such absorption and PL spectra trends indicate the degradation of both constituents (CdSe and CdS) in NR heterostructure. After 4 cycles in photocatalytic tests, noticeable changes of CdSe/CdS NRs can be observed in TEM images (Fig. 5b). The rods become shorter and narrower. The elemental mapping data obtained for CdSe/CdS NRs before and after 4 photocatalytic cycles indicate the degradation of the CdSe seeds, as evidenced by significantly lower concentrations of Se in the NR volumes (Fig. 5e and 5f). Therefore, TEM data support the optical data regarding degradation of both CdSe and CdS.

Conclusions

Our study demonstrated that CdSe/CdS NRs can catalyze the oxidative S-S coupling reaction in an organic solvent under aerobic conditions with a very high efficiency, i.e. disulfide formation at 87% yield with an extremely low concentration of catalyst loading (~1.5×10^{-4} mol%). We demonstrate that primary amines play an important role in the transformation of the thiols into corresponding disulfide in nonpolar solvents. The reaction between thiols and amines in organic solvent leads to the formation of thiolates, which have lower redox potentials and, hence, can be easier oxidized. Based on the optical spectroscopy data and EPR studies, We show that there are two parallel pathways that are responsible for the aerobic oxidation of thiophenol into disulfide in the presence of primary amines: (i) direct oxidation of photoexcited form of thiolate by oxygen resulting in the formation of disulfide, and (ii) oxidation of thiolate by photogenerated holes from CdSe/CdS NRs. The EPR data indicate that the same reactive intermediates are responsible for both reaction pathways. Charge separation characteristics of CdSe/CdS NRs make them better photocatalysts than CdSe NCs because the lifetime of photogenerated holes and electrons are much longer in NRs, making them readily available for extraction.

Most of the previous photocatalytic studies on semiconductor NCs were focused on utilization of photogenerated electrons in water, mainly for H_2 generation. Thiols were only used as sacrificial hole scavengers or to preserve the optical properties of semiconductor NCs in water.[26, 72] While the thiolate formation in aqueous media can be controlled by pH, photocatalytic conversion of thiol into disulfide in water has limited applications because of the low solubility of organic thiols. The utilization of organic solvents in which organic thiols have much better solubilities thus opens new opportunities for carrying out this type of coupling chemistry. We show that thiolates can be used for a rather efficient scavenger of holes photogenerated in semiconductor NCs to yield valuable organic molecules in nonpolar media.

Experimental

Materials: CdO (Sigma-Aldrich, 99%), *n*-propylphosphonic acid (PPA, Sigma-Aldrich, 95%), trioctylphosphine oxide (TOPO, Sigma-Aldrich, 99%), octadecylphosphonic acid (ODPA, PCI Synthesis, 97%), trioctylphosphine (TOP, Fluka, 90%), selenium (Aldrich, 98%), sulfur (Sigma-Aldrich, 99%), *n*-octylamine (Aldrich, 99%), thiophenol (Sigma-Aldrich, 99%), phenyl disulfide (Sigma-Aldrich, 99%), biphenyl (Sigma-Aldrich, 99%), toluene (Sigma-Aldrich, anhydrous, 99.8%), methanol (Sigma-Aldrich, for HPLC, 99.9%), alcohol (Fischer Scientific, 89-91%), acetone (Fischer Scientific, 99.5%) were used as received.

Synthesis of CdSe quantum dots.[10] CdO (60.0 mg), TOPO (3.0 g) and ODPA (0.28 g) were mixed in a dry 50 mL round bottom flask, and kept under vacuum at 150 °C for ~ 1 hour. After that, the reaction mixture was heated up to 300 °C resulting in

dissolution of CdO and formation of a transparent and colorless solution. TOP (1.5 g) was injected into the flask and the temperature was increased up to 370 °C at which the Se-TOP solution (58.0 mg Se + 0.36 g TOP) was injected rapidly into the hot solution. The reaction was stopped by removing the heating mantle and quenched in room-temperature water bath only after 1 minute. After cooling to the room temperature, the CdSe NCs were precipitated with methanol and dissolved in toluene. The same process was repeated several times to remove excess ligand. The NCs using in photocatalytic tests were dissolved in toluene and CdSe NCs further used in synthesis of CdSe/CdS were dissolved in TOP. The concentration of CdSe NCs solution was determined by optical absorption experiments using Beer-Lambert Law. The extinction coefficient of CdSe NCs was calculated by the first excitonic absorption peak wavelength and particle size.[73]

Synthesis of CdSe/CdS nanorods.[9] CdO (0.207 g), ODPA (1.08 g), PPA (15.0 mg) and TOPO (3.35 g) were mixed in a 50 ml dry round bottom flask and kept at ~150 °C for 1.5 hours under vacuum. Then the mixture was heated to 340 °C under N2 flow to fully dissolve the CdO (a clear and colorless solution is formed). After that, TOP (1.5 g) was injected into the flask and the solution was heated up to 340 °C. In the meantime, S-TOP solution was prepared by dissolving sulfur (51.5 mg) in TOP (0.6 g) at 50 °C under N_2. The S-TOP solution was rapidly injected into the flask at 340 °C, and 20 s later CdSe NCs (~6 mg) dissolved in TOP were injected. The reaction temperature dropped down to 320 °C and the synthesis was allowed to continue for 10 minutes and stopped by the injection of 10 mL of anhydrous toluene and the removal of heating mantle. Once the solution was cooled down to room temperature, CdSe/CdS NRs were isolated by diluting the crude solution with an equivalent volume of toluene followed by adding ethanol. The precipitation was separated by centrifugation and re-dispersed in toluene. The process was repeated three times in order to remove excessive ligands. The final CdSe/CdS NRs were dissolved in toluene. The concentration of CdSe/CdS NRs was determined by optical absorption experiments using Beer-Lambert Law and the extinction coefficient of CdSe/CdS NRs was calculated according to method described before.[74]

General procedure for photocatalytic oxidative coupling of thiophenol. In a dry glass vial with a stir bar, thiophenol (0.2 mmol, 0.1 M), *n*-octylamine (0.2 mmol, 0.1 M) and CdSe/CdS NRs (3×10^{-7} mmol, 1.5×10^{-7} M) were dissolved in 2.0 mL anhydrous toluene under ambient conditions. The solution was stirred at room temperature under blue LED irradiation (415 nm, 14.4 mV) for 2 hours. After the reaction, 2.0 mL acetone was added to the solution to separate the CdSe/CdS NRs. The mixture was centrifuged at 10,000 rpm for 5 minutes. The supernatant was collected, and the precipitates were re-dissolved in toluene for further experiments.

Characterization Methods. GC-MS analysis was conducted on Agilent 7890A and 5975C instrument using 99.999% helium as a carrier gas. We used different concentration of biphenyl to obtain a calibration curve, and use it as an internal standard for GC-MS analysis.

TEM images were obtained using JEOL JEM-2100F equipped with a Gatan GIF Quantum Energy Filters and an Oxford X-MaxN 80 TLE detector and operated at 200 kV. STEM images and elemental mappings were obtained using FEI Talos F200X TEM/STEM equipped with a SuperX energy-dispersive spectrometer.

The XRD data were obtained using Bruker D2 Phaser using Cu K (alpha) radiation.

The X-ray photoelectron spectroscopy (XPS) spectra were collected for a film deposited on Si substrate by evaporation of toluene solution of CdSe/CdS NRs on a Thermo K-Alpha XPS system with a spot size of 400 μm and a resolution of 0.1 eV. Samples were etched with Ar^+ sputtering at a rate of 0.05 nm/sec. All spectra were processed using Thermo Avantage, which is a software package provided through ThermoScientific.

UV-Vis spectra were obtained on Varian Cary 50 spectrophotometer, using a quartz cuvette with a 1.0-cm optical length and a 2.5-mm optical length. The PL spectra were collected using a Nanolog instrument from Horiba Instruments Inc., equipped with a 450 W intense broadband CW xenon lamp, a double-grating excitation monochromator with gratings at blazed at 500 nm with 1,200 lines/mm.

Ultrafast transient absorption measurements were carried out using an amplified Ti:Sapphire laser (800 nm, 35 fs, 2 kHz repetition rate) the output of which was split into two beams. The first beam, containing 10% of the power, was focused into a sapphire window to generate a white light continuum (440 nm – 750 nm), which serves as the probe. The other beam, containing 90% of the power, was sent into an optical parametric amplifier to generate the 400-nm pump beam. The pump beam is attenuated with neutral density filters, focused, and overlapped with the probe beam at the sample. The pump fluence was chosen to be < 10 $\mu J/cm^{-2}$; at these pump energies, we observed no power-dependent kinetic features corresponding to multiexciton decay, indicating that each nanorod absorbs on average less than one photon per pulse.

PL decay measurements were recorded for rapidly stirred nanorod solutions in toluene solvent. Nanorods were excited at 2 kHz by 400-nm pulses from a 2 kHz amplified Ti:sapphire laser. The PL was collected with a lens and directed through a long pass filter (435 nm), a 150-mm spectrograph, and detected with a photo*n*-counting streak camera. The pump fluence was chosen to be < 10 $\mu J/cm^{-2}$ and no power-dependent behavior was observed. It is worth mention that the UV exposure condition of samples did not negatively affect PL decay measurements despite additional PL from the sample.

X-band (9.5 GHz) EPR experiments were performed using a continuous-wave (cw) Bruker Elexsys II E500 spectrometer (Bruker Biospin Corp., Rheinstetten, Germany) equipped with a TE102 rectangular EPR resonator (Bruker ER 4102ST). Measurements at cryogenic temperatures (10 K, 50 K and 80 K) were conducted at helium gas-flow cryostat (ICE Oxford, UK). The samples were loaded in 4 mm o.d. quartz tubes, frozen in liquid nitrogen, and transferred to the pre-cooled resonator. The EPR spectra were recorded under 30-40 mW laser

illumination (OPO, BasiScan from GWU, pumped by a Nd:YAG laser (Quanta-Ray INDI, Spectra Physics).

Conflicts of interest

There are no conflicts to declare.

Acknowledgements

Use of the Center for Nanoscale Materials, an Office of Science user facility, and the work at the Chemical Sciences and Engineering Division were supported by the U.S. Department of Energy, Office of Science, Office of Basic Energy Sciences, and Division of Chemical Sciences, Geosciences, and Biosciences under Contract No. DE-AC0206CH-11357. The research effort of Y. Sha was supported by a scholarship from the China Scholarship Council (CSC) (201706270410). A. Lei acknowledge the support from the National Natural Science Foundation of China (21520102003), the Hubei Province Natural Science Foundation of China (2017CFA010), and the Program of Introducing Talents of Discipline to Universities of China (111 Program).

References

1. K. Nakata and A. Fujishima, *Journal of Photochemistry and Photobiology C: Photochemistry Reviews*, 2012, **13**, 169-189.
2. L. Cheng, Q. Xiang, Y. Liao and H. Zhang, *Energy & Environmental Science*, 2018, **11**, 1362-1391.
3. F. Qiu, Z. Han, J. J. Peterson, M. Y. Odoi, K. L. Sowers and T. D. Krauss, *Nano Letters*, 2016, **16**, 5347-5352.
4. M. B. Wilker, K. J. Schnitzenbaumer and G. Dukovic, *Isr. J. Chem.*, 2012, **52**, 1002-1015.
5. P. Moroz, A. Boddy and M. Zamkov, *Frontiers in Chemistry*, 2018, **6**, Article 353.
6. Z.-R. Tang, B. Han, C. Han and Y.-J. Xu, *Journal of Materials Chemistry A*, 2017, **5**, 2387-2410.
7. S. Liu, Z.-R. Tang, Y. Sun, J. C. Colmenares and Y.-J. Xu, *Chemical Society Reviews*, 2015, **44**, 5053-5075.
8. Z. Zhang, K. Edme, S. Lian and E. A. Weiss, *Journal of the American Chemical Society*, 2017, **139**, 4246-4249.
9. D. V. Talapin, J. H. Nelson, E. V. Shevchenko, S. Aloni, B. Sadtler and A. P. Alivisatos, *Nano Letters*, 2007, **7**, 2951-2959.
10. L. Carbone, C. Nobile, M. De Giorgi, F. D. Sala, G. Morello, P. Pompa, M. Hytch, E. Snoeck, A. Fiore, I. R. Franchini, M. Nadasan, A. F. Silvestre, L. Chiodo, S. Kudera, R. Cingolani, R. Krahne and L. Manna, *Nano Letters*, 2007, **7**, 2942-2950.
11. K. Wu, L. J. Hill, J. Chen, J. R. McBride, N. G. Pavlopolous, N. E. Richey, J. Pyun and T. Lian, *ACS Nano*, 2015, **9**, 4591-4599.
12. C. She, A. Demortière, E. V. Shevchenko and M. Pelton, *The Journal of Physical Chemistry Letters*, 2011, **2**, 1469-1475.
13. C. She, G. W. Bryant, A. Demortière, E. V. Shevchenko and M. Pelton, *Physical Review B*, 2013, **87**, 155427.
14. V. L. Bridewell, R. Alam, C. J. Karwacki and P. V. Kamat, *Chemistry of Materials*, 2015, **27**, 5064-5071.
15. Y. Yang, K. Wu, A. Shabaev, A. L. Efros, T. Lian and M. C. Beard, *ACS Energy Letters*, 2016, **1**, 76-81.
16. Y. Ben-Shahar, F. Scotognella, I. Kriegel, L. Moretti, G. Cerullo, E. Rabani and U. Banin, *Nature Communications*, 2016, **7**, 10413.
17. R. Bera, A. Dutta, S. Kundu, V. Polshettiwar and A. Patra, *The Journal of Physical Chemistry C*, 2018, **122**, 12158-12167.
18. B. Chica, C.-H. Wu, Y. Liu, M. W. W. Adams, T. Lian and R. B. Dyer, *Energy & Environmental Science*, 2017, **10**, 2245-2255.
19. M. J. Berr, P. Wagner, S. Fischbach, A. Vaneski, J. Schneider, A. S. Susha, A. L. Rogach, F. Jäckel and J. Feldmann, *Applied Physics Letters* 2012, **100**, 223903.
20. K. Wu, Z. Chen, H. Lv, H. Zhu, C. L. Hill and T. Lian, *Journal of the American Chemical Society*, 2014, **136**, 7708-7716.
21. L. Amirav and A. P. Alivisatos, *The Journal of Physical Chemistry Letters*, 2010, **1**, 1051-1054.
22. P. Kalisman, Y. Nakibli and L. Amirav, *Nano Letters*, 2016, **16**, 1776-1781.
23. A. K. Simlandy, B. Bhattacharyya, A. Pandey and S. Mukherjee, *ACS Catalysis*, 2018, **8**, 5206-5211.
24. H. B. Chandrashekar, A. Maji, G. Halder, S. Banerjee, S. Bhattacharyya and D. Maiti, *Chem Commun (Camb)*, 2019, **55**, 6201-6204.
25. J. A. Caputo, L. C. Frenette, N. Zhao, K. L. Sowers, T. D. Krauss and D. J. Weix, *Journal of the American Chemical Society*, 2017, **139**, 4250-4253.
26. K. P. McClelland and E. A. Weiss, *ACS Applied Energy Materials*, 2018, **2**, 92-96.
27. K. Wu, Y. Du, H. Tang, Z. Chen and T. Lian, *Journal of the American Chemical Society*, 2015, **137**, 10224-10230.
28. M. V. Trivedi, J. S. Laurence and T. J. Siahaan, *Curr Protein Pept Sci*, 2009, **10**, 614-625.
29. B. Heras, M. Kurz, S. R. Shouldice and J. L. Martin, *Curr Opin Struct Biol*, 2007, **17**, 691-698.
30. R. J. W. Cremlyn and R. J. Cremlyn, *An introduction to organosulfur chemistry*, Wiley New York, 1996.
31. D. H. Dethe, A. Srivastava, B. D. Dherange and B. V. Kumar, *Advanced Synthesis & Catalysis*, 2018, **360**, 3020-3025.
32. M. Oba, K. Tanaka, K. Nishiyama and W. Ando, *J Org Chem*, 2011, **76**, 4173-4177.
33. K. Y. D. Tan, G. F. Teng and W. Y. Fan, *Organometallics*, 2011, **30**, 4136-4143.
34. A. Talla, B. Driessen, N. J. W. Straathof, L.-G. Milroy, L. Brunsveld, V. Hessel and T. Noël, *Advanced Synthesis & Catalysis*, 2015, **357**, 2180-2186.
35. T. Tankam, K. Poochampa, T. Vilaivan, M. Sukwattanasinitt and S. Wacharasindhu, *Tetrahedron*, 2016, **72**, 788-793.
36. D. J. Cole-Hamilton, *Science*, 2003, **299**, 1702-1706.
37. X.-B. Li, Z.-J. Li, Y.-J. Gao, Q.-Y. Meng, S. Yu, R. G. Weiss, C.-H. Tung and L.-Z. Wu, *Angewandte Chemie International Edition*, 2014, **53**, 2085-2089.
38. W.-B. Wu, Y.-C. Wong, Z.-K. Tan and J. Wu, *Catalysis Science & Technology*, 2018, **8**, 4257-4263.
39. K. Nose, H. Fujita, T. Omata, S. Otsuka-Yao-Matsuo, H. Nakamura and H. Maeda, *Journal of Luminescence*, 2007, **126**, 21-26.
40. L. A. H. van Bergen, G. Roos and F. De Proft, *The Journal of Physical Chemistry A*, 2014, **118**, 6078-6084.
41. A. Zeida, R. Babbush, M. C. González Lebrero, M. Trujillo, R.

Radi and D. A. Estrin, *Chemical Research in Toxicology*, 2012, **25**, 741-746.
42. D. A. Hines and P. V. Kamat, *ACS Appl Mater Interfaces*, 2014, **6**, 3041-3057.
43. I. S. Liu, H.-H. Lo, C.-T. Chien, Y.-Y. Lin, C.-W. Chen, Y.-F. Chen, W.-F. Su and S.-C. Liou, *Journal of Materials Chemistry*, 2008, **18**, 675–682
44. Z.-J. Jiang, V. Leppert and D. F. Kelley, *The Journal of Physical Chemistry C*, 2009, **113**, 19161-19171.
45. K. P. Acharya, R. S. Khnayzer, T. O'Connor, G. Diederich, M. Kirsanova, A. Klinkova, D. Roth, E. Kinder, M. Imboden and M. Zamkov, *Nano Lett*, 2011, **11**, 2919-2926.
46. A. De, N. Mondal and A. Samanta, *The Journal of Physical Chemistry C*, 2018, **122**, 13617-13623.
47. A. Demortière, R. D. Schaller, T. Li, S. Chattopadhyay, G. Krylova, T. Shibata, P. C. dos Santos Claro, C. E. Rowland, J. T. Miller, R. Cook, B. Lee and E. V. Shevchenko, *Journal of the American Chemical Society*, 2014, **136**, 2342-2350.
48. J. Huang, D. Stockwell, Z. Huang, D. L. Mohler and T. Lian, *J Am Chem Soc*, 2008, **130**, 5632-5633.
49. K. Tvrdy, P. A. Frantsuzov and P. V. Kamat, *Proc Natl Acad Sci U S A*, 2011, **108**, 29-34.
50. F. Scholz, L. Dworak, V. V. Matylitsky and J. Wachtveitl, *Chemphyschem*, 2011, **12**, 2255-2259.
51. F. G. Bordwell, X.-M. Zhang, A. V. Satish and J. P. Cheng, *Journal of the American Chemical Society*, 1994, **116**, 6605-6610.
52. F. Denes, M. Pichowicz, G. Povie and P. Renaud, *Chem Rev*, 2014, **114**, 2587-2693.
53. P. S. H. Bolman, I. Safarik, D. A. Stiles, W. J. R. Tyerman and O. P. Strausz, *Canadian Journal of Chemistry*, 1970, **48**, 3872-3876.
54. D. P. Nair, M. Podgórski, S. Chatani, T. Gong, W. Xi, C. R. Fenoli and C. N. Bowman, *Chemistry of Materials*, 2014, **26**, 724-744.
55. A. A. Oswald, F. Noel and A. J. Stephenson, *The Journal of Organic Chemistry*, 1961, **26**, 3969-3974.
56. H. J. Kim, J. H. Yoon and S. Yoon, *J Phys Chem A*, 2010, **114**, 12010-12015.
57. T. J. Wallace, N. Jacobson and A. Schriesheim, *Nature*, 1964, **201**, 609-610.
58. K. A. Ogawa and A. J. Boydston, *Organic Letters*, 2014, **16**, 1928-1931.
59. B. K. Pong, B. L. Trout and J. Y. Lee, *Langmuir*, 2008, **24**, 5270-5276.
60. B. T. Diroll, M. E. Turk, N. Gogotsi, C. B. Murray and J. M. Kikkawa, *ChemPhysChem*, 2016, **17**, 759-765.
61. M. L. Pegis, J. A. S. Roberts, D. J. Wasylenko, E. A. Mader, A. M. Appel and J. M. Mayer, *Inorganic Chemistry*, 2015, **54**, 11883-11888.
62. A. Dhakshinamoorthy, M. Alvaro and H. Garcia, *Chemical Communications*, 2010, **46**, 6476-6478.
63. I. Funes-Ardoiz and F. Maseras, *ACS Catalysis*, 2018, **8**, 1161-1172.
64. S. Siahrostami, G.-L. Li, V. Viswanathan and J. K. Nørskov, *The Journal of Physical Chemistry Letters*, 2017, **8**, 1157-1160.
65. K. Jiang, S. Back, A. J. Akey, C. Xia, Y. Hu, W. Liang, D. Schaak, E. Stavitski, J. K. Nørskov, S. Siahrostami and H. Wang, *Nature Communications*, 2019, **10**, 3997.
66. D. W. Flaherty, *ACS Catalysis*, 2018, **8**, 1520-1527.
67. E. Jung, H. Shin, W. Hooch Antink, Y.-E. Sung and T. Hyeon, *ACS Energy Letters*, 2020, **5**, 1881-1892.
68. Z. Lu, G. Chen, S. Siahrostami, Z. Chen, K. Liu, J. Xie, L. Liao, T. Wu, D. Lin, Y. Liu, T. F. Jaramillo, J. K. Nørskov and Y. Cui, *Nature Catalysis*, 2018, **1**, 156-162.
69. N. Waiskopf, Y. Ben-Shahar, M. Galchenko, I. Carmel, G. Moshitzky, H. Soreq and U. Banin, *Nano Letters*, 2016, **16**, 4266-4273.
70. J. H. Walton and H. A. Lewis, *Journal of the American Chemical Society*, 1916, **38**, 633-638.
71. B. Cardey, S. Foley and M. Enescu, *The Journal of Physical Chemistry A*, 2007, **111**, 13046-13052.
72. S. Jeong, M. Achermann, J. Nanda, S. Ivanov, V. I. Klimov and J. A. Hollingsworth, *Journal of the American Chemical Society*, 2005, **127**, 10126-10127.
73. W. W. Yu, L. Qu, W. Guo and X. Peng, *Chemistry of Materials*, 2003, **15**, 2854-2860.
74. D. V. Talapin, R. Koeppe, S. Götzinger, A. Kornowski, J. M. Lupton, A. L. Rogach, O. Benson, J. Feldmann and H. Weller, *Nano Letters*, 2003, **3**, 1677-1681.